Change in total angular momentum within the $z\ ^3F^\circ$ titanium excited state induced by collisions with ground-state argon, neon, and helium atoms

D. Dezert and V. Quichaud
Equipe Thermodynamique et Plasmas, Université de Limoges, 123 Albert Thomas Avenue, 87060 Limoges Cedex, France

D. Degout
Etablissement Technique Central de L'Armement 16 bis, Prieur de la Côte d'Or Avenue, 94114 Arceuil Cedex, France

A. Catherinot
Equipe Thermodynamique et Plasmas, Université de Limoges, 123 Albert Thomas Avenue, 87060 Limoges Cedex, France

(Received 11 April 1986)

Collisions that produce a change in the total angular momentum and quenching processes involving the triplet $z\ ^3F^\circ$ titanium excited level and noble gases have been studied by laser perturbation and time-resolved spectroscopy. Titanium atoms are produced in a hollow-cathode discharge, and the analysis of resonance and sensitized fluorescence light decays enable us to determine total-angular-momentum-changing (J-changing) and quenching cross sections induced by collisions with helium, neon, and argon atoms. The thermally averaged J-changing cross section ($z\ ^3F_i^\circ \rightarrow z\ ^3F_j^\circ$) in units of 10^{-16} cm^2 are $\bar{\sigma}_{4\rightarrow 2}=1.7\pm0.5$, 0.7 ± 0.06, 3.1 ± 1; $\bar{\sigma}_{4\rightarrow 3}=11\pm2$, 1.4 ± 0.1, 11 ± 1; $\bar{\sigma}_{3\rightarrow 2}=7\pm2$, 2.2 ± 0.3, 14 ± 2, respectively, for helium, neon, and argon colliding partners. As for alkali-metal—noble-gas collisions, a pronounced minimum of the J-changing cross sections is obtained for the titanium ($z\ ^3F^\circ$)—neon collisions. Radiative destruction probabilities of the $z\ ^3F_j^\circ$ ($j=4,3,2$) titanium sublevels have been measured also, and good agreement with accepted values is found.

I. INTRODUCTION

These last few years, numerous studies have been performed on elementary processes involving metal vapors which are interesting from a fundamental point of view and for applications in physics and chemical physics. These studies have been developed essentially in two directions.

On the one hand, accurate values of excited-state radiative lifetimes have been measured by time-resolved laser-induced-fluorescence methods with emphasis on refractory metal species. Different sources of vapors are used: atomic beams[1,2] or ion beams[3,4] produced from cathodic sputtering in rare-gas discharges or from electrically heated crucibles,[5] laser ablation of a metallic target as proposed by Measures *et al.*[6] for atomic species, and by Bondybey *et al.*[7] for clusters.

On the other hand, many studies have been done on thermal-energy charge-transfer processes and Penning ionization reactions involving metal vapor and rare gases [Cu-He,[8] Cu-Ne,[9] Zn-He,[10] and Ti-Ar (Ref. 11)], which are interesting for the understanding of metal-vapor laser action.

Beside these works, quenching mechanisms and excitation transfer processes involving metal atoms in excited states and rare gases or molecules in the ground states remain poorly studied at the present time. Indeed, though experiments have been done on metal atoms such as Cd,[12] Hg,[13] Zn,[14] and Pb,[15] to our knowledge, no data have been published on refractory metal atoms, despite their potential use for the diagnostics of metallic impurities in gases or plasmas by laser-induced-fluorescence methods,[16] for analysis of refractory metal species produced from surfaces, either by laser ablation[17] or by ion-beam sputtering,[18,19] and for understanding and modeling of new metal-vapor laser media or reactors used for deposition of refractory metal compounds.

On the contrary, these latter elementary processes have been extensively studied both theoretically[20–22] and experimentally[23–27] for alkali-metal atoms, with emphasis on fine-structure-changing collisions and mixing,[28–33] on highly excited states (Rydberg states), n-changing collisions,[34] and l-changing collisions,[35–38] induced by alkali-metal atoms in ground state, rare gases, and diatomic molecules.

This lack of experimental data concerning these elementary processes for refractory metal atoms results certainly from the difficulty in producing these species in sufficient amounts and in well-defined and reproducible conditions.

In this paper, we present new experimental results dealing with quenching mechanisms and fine-structure-changing collisions involving the $z\ ^3F_j^\circ$ [$3d^2(^3F)$-$4s\,4p(^3P^\circ)$] sublevels of titanium and the rare-gas atoms: argon, neon, and helium. In this experiment titanium atoms are produced by sputtering in a hollow-cathode discharge and they are injected in a pressure-controlled observation chamber. Then quenching mechanisms and fine-structure-changing collisions are studied by selective laser excitation and time-resolved spectroscopy. Reaction

rates are deduced from fluorescence light relaxation curves using a numerical "identification" method derived from the method previously used for helium.[39,40]

II. EXPERIMENT

The experimental apparatus is schematically shown in Fig. 1. The hollow cathode discharge, derived from the device proposed by Ohebsian *et al.*,[11] is composed of an assembly of cylindrical Macor (Corning) insulators enclosing a copper ring anode and a titanium hollow cathode (4 mm diameter). The gap between the electrodes is 28 mm.

The sputtered titanium atoms are ejected together with the buffer-gas atoms (argon or neon) into the observation chamber, leading to a green afterglow expanding jet. The stainless-steel observation chamber (500 mm long, 150 mm diameter) is equipped with fused silica windows (80 mm diameter), allowing spectroscopic investigations along two perpendicular axes at right angles to the expanding jet. A constant gas flow is obtained by means of a 35-m^3/h pump (Alcatel) and mass-flow-rate controllers (Tylan). Satisfactory titanium sputtering conditions in the hollow-cathode discharge are obtained for buffer-gas flow rates (argon or neon) in the range 200 to 1000 cm^3 min^{-1} (STP). The corresponding pressure values, measured by a capacitance manometer (MKS Baratron 222), stand between 0.4 and 2 mb. For higher pressure values of argon or neon, an auxiliary gas flow is directly injected into the observation chamber and for the studies involving helium atoms, a fixed flow rate of argon gas is injected into the hollow cathode discharge to obtain sputtered titanium atoms and helium gas is injected directly into the observation chamber.

Sputtering of the titanium cathode becomes efficient for discharge current intensities higher than 15 mA. The discharge voltage lies at about 350 V.

In all the experiments, high-purity-grade gases are used (Air Liquide 99.9995%) and the hollow cathode consists of 99.9% pure polycrystalline titanium. Between each experiment, the whole device is maintained down to a pressure of 10^{-7} mb by secondary pumping.

Laser perturbation studies have been achieved 15 cm downstream from the cathode exit hole. In this region, the light emission from the expanding jet is very weak and the species inside the medium may be considered mainly as rare gases (buffer plus auxiliary gas) and titanium atoms, in ground and metastable states.

A nitrogen-laser-pumped tunable dye laser (spectral width 0.4 Å, pulse width 1 ns, energy per pulse 2 μJ, repetition rate 20 Hz; EG&G, Princeton Applied Research PAR 2100 Dyescan) is used to selectively populate a fine-structure sublevel of the $z\ ^3F^\circ$ titanium state from the $a\ ^3F$ ground state. The laser-induced fluorescence light emission, observed at right angles to both the laser beam and the jet axis, is imaged by a fused silica lens ($f=200$ mm) with a magnification of unity onto the entrance slit of a 100-cm grating spectrometer (THR 1000, Jobin-Yvon, resolving power $\simeq$ 100 000), equiped with a RCA 7265 photomultiplier tube (rise time, 2 ns). Then the time dependence of the output signal is analyzed by a Boxcar averager (EG&G PAR 4400, gated integrator 4422, gate width equal to 2 ns), synchronized with the laser pulse and connected to a desktop computer.

Great care is taken to prevent saturation of the electronic devices by fluorescence light and stray laser light, and the laser beam is collimated and attenuated by neutral-density filters in order to reduce the interaction volume and also to eliminate laser- and population-induced phenomena such as superradiance or superfluorescence. Finally, each relaxation curve corresponds to an average of about 5000 laser shots.

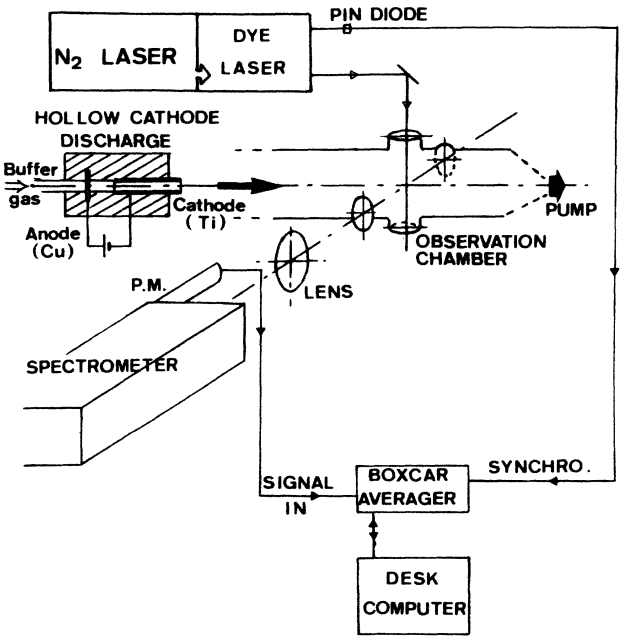

FIG. 1. Schematic diagram of the experimental apparatus.

III. MEASUREMENTS

Before the laser-perturbation studies, detailed spectroscopic investigations of the expanding jet have been undertaken along the jet axis to determine the characteristic parameters of the medium and the optimal working conditions of the hollow-cathode discharge. In particular, no traces of impurities have been spectroscopically detected. We just present in the following the results of interest obtained 15 cm downstream from the cathode exit hole, where laser perturbation studies have been carried out.

A. Characteristics of the medium in the region of laser-perturbation studies

As previously quoted, the emission of light from this region of the expanding jet is very weak and the species inside the medium are mainly rare-gas and titanium atoms, in ground and metastable states.

Population densities on the three $a\ ^3F_j$ titanium ground-state sublevels have been measured by classical absorption spectroscopy, using a titanium standard hollow-cathode lamp (Oriel). The inferred radially averaged concentration values are shown in Figs. 2(a) and 2(b), respectively, for argon and neon buffer gases, as functions of the

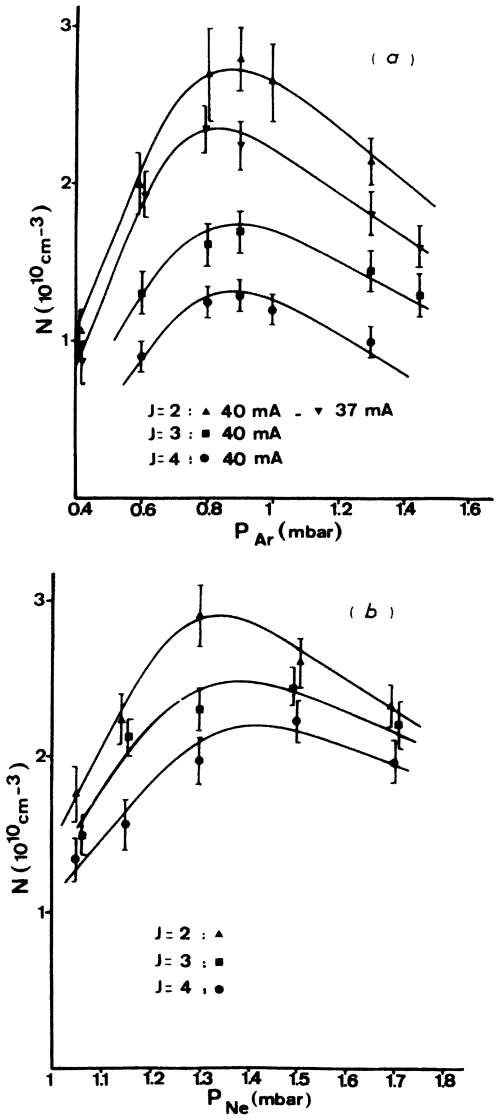

FIG. 2. Measured population densities on the three $a\,^3F_j$ titanium ground-state sublevels in the region of laser-perturbation studies (15 cm downstream from the cathode exit hole), as functions of buffer-gas pressure P in the observation chamber $I_d=40$ mA: (a) argon buffer gas, (b) neon buffer gas.

pressure P in the observation chamber (discharge current intensity $I_d=40$ mA). These values are calculated[41,42] taking into account the "apparent" diameter of the expanding jet (about 2 cm in the region under study for $P_{Ar}=0.8$ mb) and a diffusion-dominated profile has been assumed for radial concentration distributions.

We observe that the maximum sputtering efficiency is obtained for a pressure value in the observation chamber of about 0.8 mb for argon gas and 1.3 mb for neon gas. As shown in Fig. 3 for argon buffer gas (P_{Ar} fixed), the titanium concentration exhibits a nearly linear dependence on discharge current intensity I_d in the range under study, in agreement with the theoretical predictions of Koch *et al.*[43] for sputtering in hollow-cathode discharges.

According to the small energy gaps between the three $a\,^3F_j$ $(j=2,3,4)$ titanium ground-state sublevels

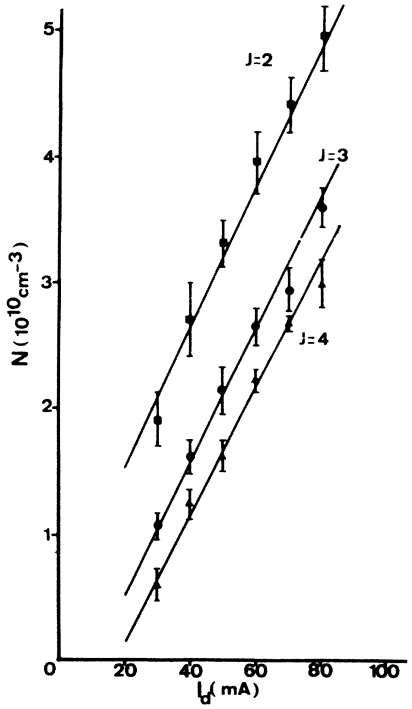

FIG. 3. Measured population densities on the three $a\,^3F_j$ titanium ground-state sublevels in the region of laser-perturbation studies, as functions of discharge current intensity I_d and for a fixed argon pressure $P_{Ar}=0.8$ mb.

$(\Delta E_{3\text{-}2}=170\ \text{cm}^{-1},\ \Delta E_{4\text{-}2}=387\ \text{cm}^{-1})$, a Boltzmann equilibrium may be assumed for the population distribution on these three sublevels, at a temperature close to the atom kinetic temperature in the expanding jet. In all cases under study (Ar and Ne buffer gases), the measured values lie in the range 400 ± 25 K.

Buffer rare-gas metastable-state population concentrations in the same region have been also measured by absorption spectroscopy using argon and neon standard lamps. As expected, we observe that metastable buffer-gas number densities have their maxima for low discharge current intensities and are lower than 5×10^8 cm^{-3} under the experimental conditions of the laser-perturbation studies ($I_d>25$ mA). As an example, population concentrations on the $^3P_0$ and $^3P_2$ metastable states of argon are shown in Fig. 4 as function of P_{Ar} for different discharge current intensities I_d. Similar results are obtained for neon.

B. Radiative destruction probabilities of the $z\,^3F^\circ_j$ $(j=2,3,4)$ titanium sublevels

A simplified energy diagram of the titanium atom is shown in Fig. 5. The experiment has been performed with argon buffer gas injected into the hollow-cathode discharge. The dye laser is tuned successively on the $a\,^3F_j$–$z\,^3F^\circ_j$ $(j=2,3,4)$ transitions and the decay of the resonance fluorescence light intensity is analyzed assuming a monoexponential relaxation law for the population variations on the considered j sublevel:

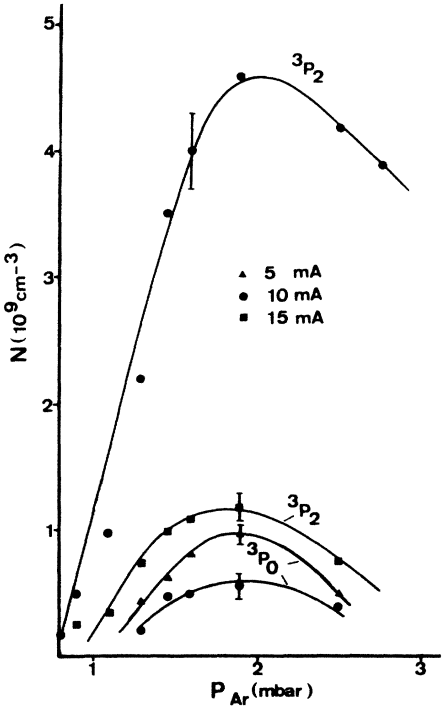

FIG. 4. Measured population densities on the $^3P_2$ and $^3P_0$ argon metastable states in the region of laser-perturbation studies as functions of argon pressure values P_{Ar} for different discharge current intensities I_d.

$$\Delta N_j(t)=\Delta N_j^0 \exp(-\Gamma_j t) . \quad (1)$$

In Eq. (1), Γ_j is the relaxation coefficient of population variations on the j sublevels depending on argon-gas pressure P_{Ar}. The Γ_j coefficients are drawn in Fig. 6 as functions of P_{Ar} for a fixed discharge current intensity ($I_d=35$ mA). Within the measurement accuracy, we observe a linear dependence on P_{Ar} of the Γ_j coefficients:

$$\Gamma_j=A_j+B_j P_{Ar} . \quad (2)$$

In Eq. (2), A_j and B_j represent, respectively, the radiative and the collisional destruction coefficients of the considered j sublevel. Though the monoexponential analysis

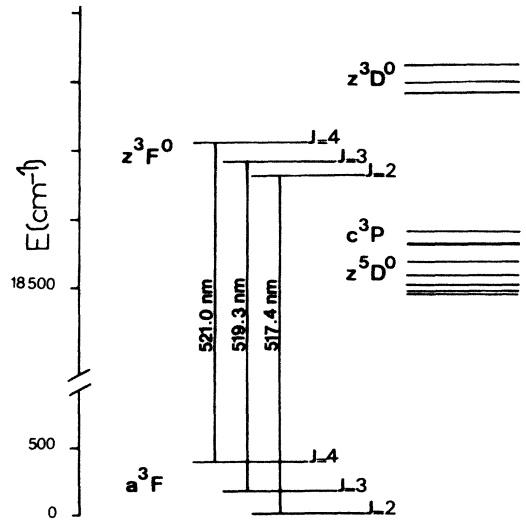

FIG. 5. Simplified energy diagram of the titanium levels involved in the experiment.

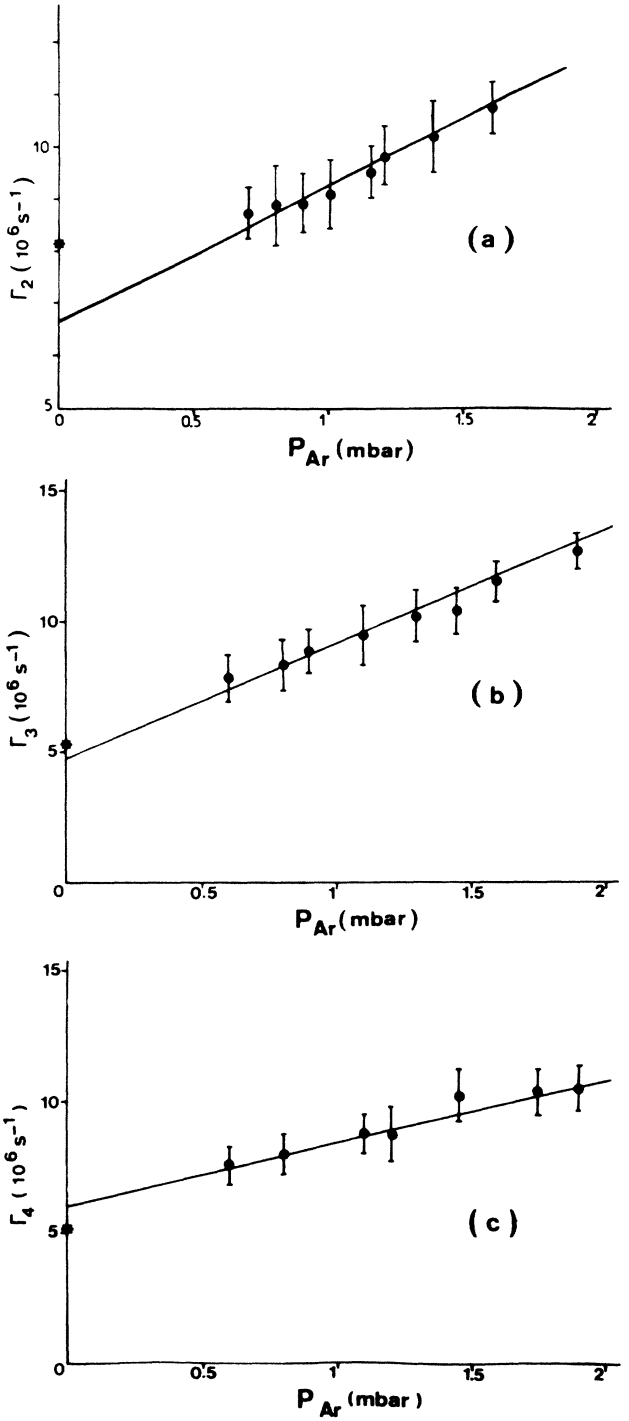

FIG. 6. Relaxation coefficient of population variation on the $z\,^3F_j^\circ$ titanium sublevel as a function of the argon gas pressure P_{Ar}: (a) $J=2$, (b) $J=3$, (c) $J=4$; * denotes A_j radiative probability of Ref. 44.

TABLE I. Radiative destruction probabilities (s^{-1}) of the $z\,^3F^\circ_j$ ($j=2,3,4$) titanium sublevels.

	$z\,^3F^\circ_{j=2}$	$z\,^3F^\circ_{j=3}$	$z\,^3F^\circ_{j=4}$
A_j (this work)	$(6.6\pm1.3)\times10^6$	$(4.8\pm1.2)\times10^6$	$(6\pm1.5)\times10^6$
A_j (Wiese *et al.* Ref. 44)	$8.19\times10^6\pm25\%$	$5.65\times10^6\pm25\%$	$5.19\times10^6\pm25\%$

of the relaxation curves is a rough approximation (see Sec. III C), extrapolation of the function $\Gamma_j=f(P_{Ar})$ to zero argon pressure allows a good estimation of the radiative coefficient A_j. The inferred A_j ($j=2,3,4$) values are summarized in Table I and they are compared to the values proposed by Wiese *et al.*[44] A good agreement is observed within the measurement accuracy.[45–47]

Several experiments have been done at constant argon pressure and for different discharge current intensities in the range 18–80 mA. This leads for instance (Fig. 2) to variations in the titanium number density of at least an order of magnitude, however, as shown in Fig. 7 for the $z\,^3F^\circ_2$ sublevel, no significant variations of the relaxation rate are observed as function of discharge current intensity.

These results indicate that the quenching processes of the $z\,^3F^\circ_j$ sublevels are mainly due to collisions with ground-state argon atoms. The other contributions (titanium atoms, argon atoms in metastable states, and charged particles) are negligibly small, according to their low concentrations in the region under study.

Moreover, these results prove that radiation trapping of the fluorescence light emitted in the resonant transitions does not affect significantly the measurements under our experimental conditions.

The same remarks remain valid when neon buffer gas is used.

C. Change in total angular momentum within the fine structure of the $z\,^3F^\circ$ titanium level induced by collisions with rare-gas atoms in ground state

The simplified diagram of the titanium levels involved in this experiment is shown in Fig. 5.

When the $z\,^3F^\circ_4$ sublevel is overpopulated by laser pulses tuned on the $a\,^3F_4$–$z\,^3F^\circ_4$ radiative transition (521.04 nm), we observe fluorescence light emission originating from the $z\,^3F^\circ_j$ ($j=4,3,2$) sublevels. The time variation of the population density of the $j=4$ sublevel is

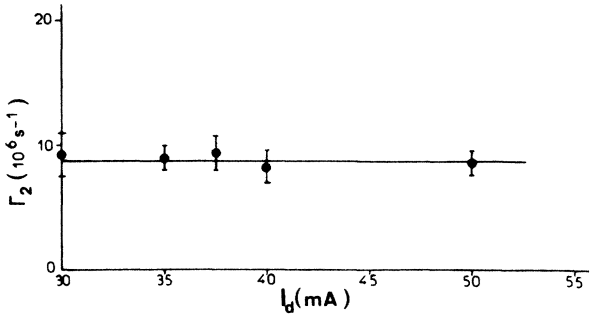

FIG. 7. Variation of the relaxation coefficient Γ_2 as a function of discharge current intensity. $P_{Ar}=1$ mb.

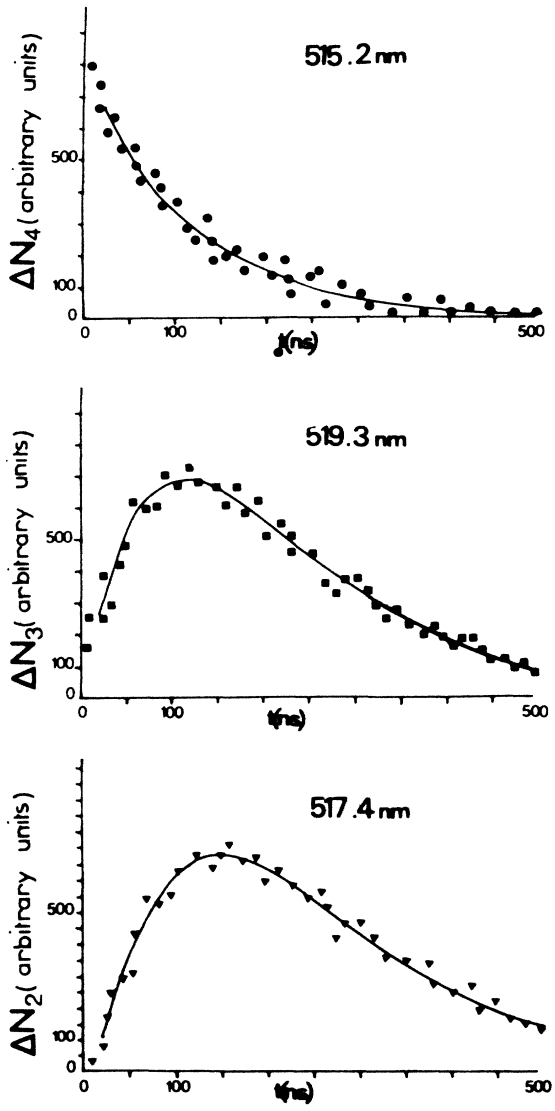

FIG. 8. Laser-induced time variations of fluorescence light intensities originating from the three $z\,^3F^\circ_j$ ($j=4,3,2$) titanium sublevels when the $z\,^3F^\circ_4$ sublevel is overpopulated by laser pulses (521.0 nm). $P_{Ar}=0.6$ mb, $I_d=40$ mA. Comparison between experimental relaxation curves [$\Delta N_j(t)$] (●, ■, ▼), and "identified" curves (——) [solutions of Eqs. (5)].

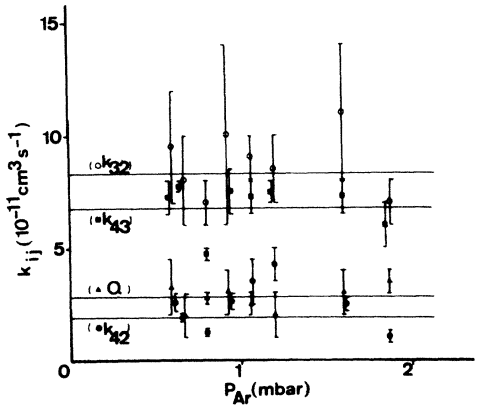

FIG. 9. J-changing k_{ij}^{Ar} and quenching Q_i^{Ar} rate coefficients obtained from the experimental results using the numerical identification method, as functions of the argon gas pressure P_{Ar}. Within the measurement accuracy $Q_4^{Ar}=Q_3^{Ar}=Q_2^{Ar}=Q^{Ar}$.

studied by observation of the fluorescence light emitted in the $z\,^3F_4^\circ$–$a\,^3F_3$ transition (515.22 nm), to avoid signal perturbation by stray laser light. Population evolutions on the $j=3$ and $j=2$ sublevels are analyzed by observation of the sensitized fluorescence light emitted, respectively, in the $z\,^3F_3^\circ$–$a\,^3F_3$ (519.29-nm) and in the $z\,^3F_2^\circ$–$a\,^3F_2$ (517.37-nm) radiative transitions. An example of the laser-induced time variations of the fluorescence light intensities originating from the three sublevels under study, is given in Fig. 8.

We observe that the relaxation curves shapes depend on the gas pressure in the observation chamber, but at a fixed pressure value, no dependence has been detected on the discharge current intensity in all cases under study. This indicates, as previously quoted, that contributions of titanium atoms, rare-gas metastable states, and charged particles to the observed excitation transfer processes are negligibly small according to their low concentration values in the region under study. Therefore, we can ascribe the observed total-angular-momentum-changing ("J-changing") excitation transfer processes to collisions with ground-state rare-gas atoms. Moreover, no fluorescence light emission has been detected originating from titanium levels other than the $z\,^3F^\circ$ triplet state under study.

Consequently, in the laser-free regime, the laser-induced population variations ΔN_j ($j=4,3,2$) may be described by the following coupled rate-equation system:[39,40]

$$\begin{aligned}
\frac{d\Delta N_4}{dt} &= -\Delta N_4\left[A_4+\sum_\alpha (k_{43}^\alpha+k_{42}^\alpha+Q_4^\alpha)N_\alpha\right] \\
&\quad +\Delta N_3\sum_\alpha k_{34}^\alpha N_\alpha+\Delta N_2\sum_\alpha k_{24}^\alpha N_\alpha\ , \\
\frac{d\Delta N_3}{dt} &= -\Delta N_3\left[A_3+\sum_\alpha (k_{34}^\alpha+k_{32}^\alpha+Q_3^\alpha)N_\alpha\right] \\
&\quad +\Delta N_4\sum_\alpha k_{43}^\alpha N_\alpha+\Delta N_2\sum_\alpha k_{23}^\alpha N_\alpha\ , \qquad (3) \\
\frac{d\Delta N_2}{dt} &= -\Delta N_2\left[A_2\sum_\alpha (k_{23}^\alpha+k_{24}^\alpha+Q_2^\alpha)N_\alpha\right] \\
&\quad +\Delta N_4\sum_\alpha k_{42}^\alpha N_\alpha+\Delta N_3\sum_\alpha k_{32}^\alpha N_\alpha\ .
\end{aligned}$$

In Eq. (3), A_j represents the total radiative destruction probability of the j sublevel (the medium is assumed optically thin, see Sec. III B), k_{ij}^α and k_{ji}^α are the forward and reverse rate coefficients of the reaction:

$$\mathrm{Ti}(z\,^3F_i^\circ)+\alpha \leftrightarrows \mathrm{Ti}(z\,^3F_j^\circ)+\alpha\ , \qquad (4)$$

and Q_j^α is the quenching rate coefficient of the j sublevel by the α collision partner of population number density N_α. In all the following experiments, we assume a complete mixing of the buffer gas and of the auxiliary gas directly injected in the reaction chamber. Numerous experiments have been achieved to improve this assumption.

1. J-changing induced by collisions with argon atoms

For the lower pressure values and up to the optimal conditions of titanium atoms production ($P_{Ar}=0.8$ mb in the observation chamber), the argon gas flow is just injected through the hollow-cathode discharge device ($F1$). For measurements performed at higher pressure values, an auxiliary argon gas flow is injected directly into the observation chamber ($F2$). Numerous tests have been carried

TABLE II. J-changing and quenching rate coefficients for the $z\,^3F_j^\circ$ ($j=2,3,4$) titanium sublevels induced by collisions with argon atoms (in 10^{-11} cm^{3}s^{-1}).

k_{43}^{Ar}	k_{42}^{Ar}	k_{32}^{Ar}	Q_4^{Ar}	Q_3^{Ar}	Q_2^{Ar}
6.7±0.7	1.9±0.8	8.3±1.8	2.8±0.4	2.8±0.4	2.8±0.4

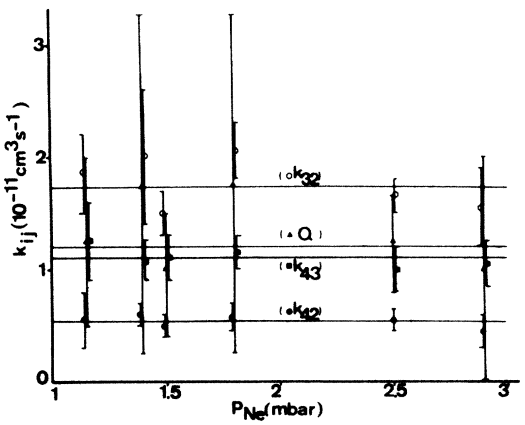

FIG. 10. J-changing k_{ij}^{Ne} and quenching Q_i^{Ne} rate coefficients obtained from the experimental results using the numerical identification method, as functions of the neon gas pressure P_{Ne}. Within the measurement accuracy $Q_4^{Ne}=Q_3^{Ne}=Q_2^{Ne}=Q^{Ne}$.

out with $F1$ alone and with $F1$ plus $F2$ to check the reproducibility of the measurements in both cases. Therefore the rate-equation system (3) may be simplified:

$$\frac{d\Delta N_i}{dt}=-\Delta N_i\left[A_i+\left[\sum_{\substack{j\\(j\neq i)}}k_{ij}^{Ar}+Q_i^{Ar}\right]N_{Ar}\right]+\sum_{\substack{j\\(j\neq i)}}\Delta N_j k_{ji}^{Ar}N_{Ar}\,,$$

$$i=4,3,2 \text{ and } j=4,3,2\,. \quad (5)$$

The dye laser is tuned to the $a\,^3F_4$–$z\,^3F_4^\circ$ (521.04-nm) transition and fluorescence light emitted in the transitions $z\,^3F_4^\circ$–$a\,^3F_3$ (515.22 nm), $z\,^3F_3^\circ$–$a\,^3F_3$ (519.29 nm), and $z\,^3F_2^\circ$–$a\,^3F_2$ (517.37 nm) is analyzed for each argon pressure value P_{Ar}. The discharge current intensity I_d is generally set to 40 mA, although measurements for $I_d=25$ and 60 mA have been done, leading to the same results at measurement accuracy.

A simplified version of the "identification" numerical method developed previously[39,40] is used to calculate the k_{ij}^{Ar} and Q_i^{Ar} rate coefficient values. The A_i radiative probabilities are those given in Table I and to reduce the number of parameters, we assume that the k_{ij}^{Ar} and k_{ji}^{Ar} rate coefficients are related by the balance equation

$$k_{ij}^{Ar}/k_{ji}^{Ar}=[(2j+1)/(2i+1)]\exp(-\Delta E_{ij}/k_BT)\,, \quad (6)$$

where $\Delta E_{ij}=E(z\,^3F_j^\circ)-E(z\,^3F_i^\circ)$. In Eq. (6) T is the atom kinetic temperature measured in Sec. III A ($T=400\pm25$ K). Taking into account these assumptions, the k_{ij}^{Ar} and Q_i^{Ar} rate coefficients are calculated such as the solutions of the rate-equation system (5) agree with the measured relaxation curves.

An example of identification is given in Fig. 8, and the inferred results for the k_{ij}^{Ar} and Q_i^{Ar} rate coefficients are shown in Fig. 9. The error bars are determined by varying the solutions of (5) within the experimental uncertainties on the relaxation curves. As expected, no influence of the discharge current intensity on the calculated values is observed. The mean values, obtained by linear regression, are presented in Table II.

2. *J-changing induced by collisions with neon atoms*

The experiment has been done in the same manner as for argon gas. For a pressure P_{Ne} in the observation chamber of lower than 1.3 mb, neon gas is just injected through the hollow-cathode discharge, and for higher pressure values, an auxiliary neon gas flow is injected directly in the observation chamber. Under the same assumptions as for argon gas, the k_{ij}^{Ne} and Q_i^{Ne} values are determined for each neon gas pressure using the numerical "identification" method. The k_{ij}^{Ne} and Q_i^{Ne} rate coefficients inferred by linear regression from the results of Fig. 10, are summarized in Table III.

3. *J-changing induced by collisions with helium atoms*

Helium gas injected into the hollow-cathode discharge does not lead to efficient titanium sputtering, according to the helium-titanium small mass ratio. Therefore, in this experiment, argon buffer gas is injected into the hollow cathode discharge up to a partial pressure $P_{Ar}=0.8$ mb corresponding to optimal sputtering conditions (see Sec. III A) and helium gas is injected directly in the observation chamber (partial pressure P_{He}). P_{Ar} and P_{He} are controlled by measuring the total pressure P in the observation chamber and the argon and helium mass-flow rates.

In this case, the rate equation system (3) reduces to:

$$\frac{d\Delta N_i}{dt}=-\Delta N_i\left[A_i+\sum_{\alpha=Ar,He}\left[\sum_{\substack{j\\(j\neq i)}}k_{ij}^{\alpha}+Q_i^{\alpha}\right]N_\alpha\right]+\sum_{\substack{j\\(j\neq i)}}\Delta N_j\left[\sum_{\alpha=Ar,He}k_{ij}^{\alpha}N_\alpha\right],$$

$$i=4,3,2;\ j=4,3,2\,. \quad (7)$$

TABLE III. J-changing and quenching rate coefficients for the $z\,^3F_j^\circ$ ($j=2,3,4$) titanium sublevels induced by collisions with neon atoms (in 10^{-11} cm^{3}s^{-1}).

k_{43}^{Ne}	k_{42}^{Ne}	k_{32}^{Ne}	Q_4^{Ne}	Q_3^{Ne}	Q_2^{Ne}
1.10±0.06	0.54±0.04	1.7±0.2	1.2±0.2	1.2±0.2	1.2±0.2

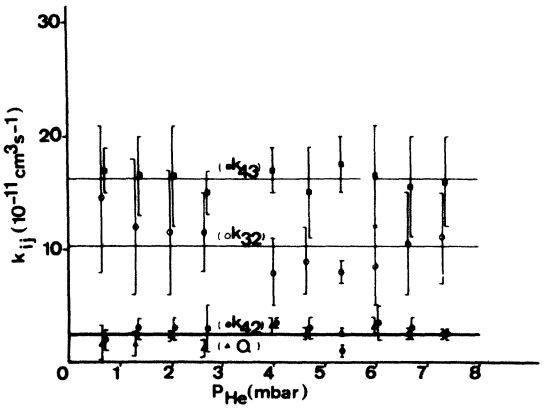

FIG. 11. J-changing k_{ij}^{He} and quenching Q_i^{He} rate coefficients obtained from the experimental results using the numerical identification method, as functions of the helium gas pressure P_{He}. Within the measurement accuracy $Q_4^{He}=Q_3^{He}=Q_2^{He}=Q^{He}$.

Then the k_{ij}^{He} and Q_i^{He} rate coefficients are calculated for each helium partial pressure P_{He} using the A_i, k_{ij}^{Ar}, and Q_i^{Ar} previously measured. They are presented in Fig. 11. The k_{ij}^{He} and Q_i^{He} rate coefficients deduced by linear regression from the results of Fig. 11 are summarized in Table IV.

IV. DISCUSSION

A. Radiative coefficients

Measurements of the radiative coefficients A_j for the $z\,^3F_j^\circ$ ($j=4,3,2$) titanium sublevels have been reported in Sec. III B. The measured A_j are summarized in Table I and they are found in good agreement with accepted values.[44]

Unfortunately, the measurement accuracy in our experiment is insufficient to discuss the suggestion of Rudolph *et al.*[5] that the transition probabilities of Ref. 44 for titanium are altered by a factor of 0.9, while the relative scale is fairly good.

Moreover, these measurements prove that radiation trapping in the resonant transitions does not affect significantly the fluorescence measurements under our experimental conditions, allowing simplifications of the rate-equation system describing the population relaxations that follow the laser perturbation.

B. J-changing and quenching processes induced by collisions with helium, neon, and argon atoms

Velocity-averaged cross sections $\bar{\sigma}_{ij}^{\alpha}$ are deduced from the k_{ij}^{α} rate coefficients given in Tables II–IV:

$$\bar{\sigma}_{ij}^{\alpha}=k_{ij}^{\alpha}/V\,, \tag{8}$$

where $V=(8RT/\pi M)^{1/2}$ is the thermal collision velocity, R is the ideal-gas constant, M the reduced mass of colliding partners, and T is the gas temperature measured in Sec. III A. We observe immediately that the quenching cross sections for a given colliding partner have the same value for the three sublevels at measurement accuracy and that the noble-gas cross sections for J-changing within the $z\,^3F^\circ$ titanium level exhibit a pronounced minimum at neon.

Due to the lack of other published measurements or theoretical calculations concerning the transition metals, the measured cross-section values can only be discussed in relation with the values obtained for other materials. For comparison, we have reported in Table V cross sections measured by different authors in alkali-metal atoms. We observe particularly that cross-section values for ^2P fine-structure-changing processes in Rb and Cs induced by collisions with helium atoms are found to be of the same order or magnitude as our results, for similar values of the reduced energy $\Delta E/k_BT$. As in our case, a minimum value of the J-changing cross sections is obtained for the neon atom as a colliding partner.

We have also reported in Table V the $7\,^2D$ and $8\,^2D$ fine-structure-mixing cross section in Rb induced by collisions with He, Ne, and Ar, measured by Supronowicz *et al.*[31] Though the proposed values are about 2 orders of magnitude larger than our results, according to the low fine-structure splitting in the $7\,^2D$ and $8\,^2D$ Rb levels, we observe still a pronounced minimum of the cross section values at neon.

For alkali-metal atoms, this behavior is ascribed to the fact that the interaction takes place essentially between the noble-gas atom and the alkali-metal valence electron, which appears to behave as a nearly free particle. This likeness between the titanium and alkali-metal J-changing cross-section behaviors as functions of the noble-gas colliding partner suggests that the semiclassical theoretical approach used for the description of J-changing processes induced in alkali-metal atoms by collision with rare gases may perhaps be extended to titanium–rare-gas collisions, at least for the excited triplet state under study [$3d^2(^3F)$-$4s\,4p(^3P^\circ)$], though open inner shells complicate *a priori* seriously the theoretical problem.

Finally, our results are compared in Table V with recent cross-section measurements[48] and calculations[49] for intramultiplet mixing in collisions of calcium ($4s\,4p\,^3P$) with helium. It is difficult to correlate these results with our measurements and we can just observe that a pronounced minimum of the cross sections is theoretically

TABLE IV. J-changing and quenching rate coefficients for the $z\,^3F_j^\circ$ ($j=2,3,4$) titanium sublevels induced by collisions with helium atoms (in 10^{-11} cm^{3}s^{-1}).

k_{43}^{He}	k_{42}^{He}	k_{32}^{He}	Q_4^{He}	Q_3^{He}	Q_2^{He}
16.3±1.2	2.6±0.7	10.3±2	2.5±0.3	2.5±0.3	2.5±0.3

TABLE V. Velocity-averaged cross sections for J-changing and quenching of the $z\,^3F_j^\circ$ titanium sublevels for collisions with helium, neon, and argon atoms in ground state. Comparison with available data.

Intramultiplet transfers Ti($z\,^3F_i^\circ \rightarrow z\,^3F_j^\circ$) (this work)	$\Delta E_{ij}/k_BT$	Cross sections (Å^2) He	Ne	Ar
4→2	0.90	1.7±0.5	0.70±0.06	3.1±1
4→3	0.55	11±2	1.4±0.1	11±1
3→2	0.36	7±2	2.2±0.3	14±2

Quenching Ti $z\,^3F_i^\circ$ (this work)	Cross sections (Å^2) He	Ne	Ar
$i=4,3,2$	1.7±0.4	1.5±0.3	4.5±0.6

Intramultiplet transfers (alkali metals)	$\Delta E_{ij}/k_BT$	Cross sections (Å^2) He	Ne	Ar
Rb $6\,^2P_{3/2}\rightarrow 6\,^2P_{1/2}$ [a]	0.26	17.1±3.6	5.6±1	13.2±2.6
Cs $7\,^2P_{3/2}\rightarrow 7\,^2P_{1/2}$ [b]	0.58	11±2	0.16±0.03	0.10±0.02
Cs $7\,^2P_{3/2}\rightarrow 7\,^2P_{1/2}$ [a]	0.81	12.8±2.6	0.047±0.01	0.075±0.02
Rb $7\,^2D_{5/2}\rightarrow 7\,^2D_{3/2}$ [c]	$\Delta E=1.51$ cm^{-1}	580±90	400±60	690±100
Rb $8\,^2D_{5/2}\rightarrow 8\,^2D_{3/2}$ [c]	$\Delta E=1.01$ cm^{-1}	580±90	320±60	940±190

Intramultiplet transfers (calcium) Ca $^3P_i^\circ\rightarrow{}^3P_j^\circ$	$\Delta E_{ij}/k_BT$	Cross sections (Å^2) He	Ne	Ar
2→1	0.35	31.9±4.2 [d], 11.2 [e]		
2→0	0.53	5.5±1.6 [d], 0.8 [e]		
1→0	0.12	2.0±5.0 [d], 2.5 [e]		

[a]Reference 33.
[b]Reference 23.
[c]Reference 31.
[d]Reference 48 (measurements).
[e]Reference 49 (theoretical calculations).

found for $\Delta J=2$,[49] in agreement with our results but in contradiction with the measurements of Ref. 48. It would be interesting to compare our results with intramultiplet mixing cross sections of calcium ($4s4p\,^3P_j$) induced by collision with neon and argon gas.

V. CONCLUSION

Fine-structure-changing collisions and quenching involving the triplet $z\,^3F^\circ$ titanium excited level and noble gases (He, Ne, Ar) have been studied by laser perturbation and time-resolved spectroscopy. Titanium atoms are produced in a home-designed hollow-cathode discharge allowing reproducible measurements. Then, analysis of resonance and sensitized fluorescence light intensity decays enable us to determine fine-structure-changing cross sections within the $z\,^3F^\circ$ titanium level induced by collisions with helium, neon, and argon atoms. As observed for alkali-metal—noble-gas collisions by different authors, we obtain a pronounced minimum of the J-changing cross-section values for neon. These results suggest that theoretical approaches developed for alkali-metal—noble-gas collisions may be perhaps extended to titanium—noble-gas collisions at least for J-changing collisions within the $z\,^3F^\circ$ titanium level under study. Unfortunately, the lack of available data on transition ele-

ments does not provide more detailed comparisons of our results with experimental or theoretical works of others. At the present time, experiments are undertaken in our laboratory to extend our measurements particularly on collisions of titanium triplet level atoms with diatomic molecules and J-changing processes in quintet titanium levels induced by collisions with rare gases. We hope that these results would stimulate calculations and other measurements on such processes.

ACKNOWLEDGMENTS

The technical assistance of M. Giraudon is gratefully acknowledged. This work was partly supported by Direction des Recherches, Etudes et Techinques (D.R.E.T.) under Contract No. 84/158. Equipe Thermodynamique et Plasmas is Unite Associe No. 320 Centre National de la Recherches Scientifique.

[1]D. W. Duquette, S. Salih, and J. E. Lawler, Phys. Rev. A **24**, 2847 (1981); **25**, 3382 (1982); **26**, 2633 (1982); S. Salih, D. W. Duquette, and J. E. Lawler, *ibid.* **27**, 1193 (1983).

[2]P. Hannaford and R. M. Lowe, Opt. Eng. **22**, 532 (1983).

[3]S. Salih and J. E. Lawler, Phys. Rev. A **28**, 3653 (1983).

[4]M. Kwiatkowski, K. Werner, and P. Zimmermann, Phys. Rev. A **31**, 2695 (1985).

[5]J. Rudolph and V. Helbig, J. Phys. B **15**, L1 (1982); **15**, L599 (1982).

[6]R. M. Measures, N. Drewell, and H. S. Kwong, Phys. Rev. A **16**, 109 (1977).

[7]V. E. Bondybey, G. P. Schwartz, and J. H. English, J. Chem. Phys. **78**, 11 (1983) (and references therein).

[8]D. W. Ernie and H. J. Oskam, Phys. Rev. A **23**, 325 (1981).

[9]Y. S. Cho, D. W. Ernie, and H. J. Oskam, Phys. Rev. A **30**, 1760 (1984).

[10]G. J. Collins, J. Appl. Phys. **44**, 10 (1973).

[11]D. Ohebsian, N. Sadeghi, C. Trassy, and J. M. Mermet, Opt. Commun. **32**, 81 (1980).

[12]M. Czajkowski, E. Walentynowicz, and L. Krause, J. Quant. Spectrosc. Radiat. Transfer **29**, 113 (1983); A. Baczynski, M. Czajkowski, and L. Krause, *ibid.* **30**, 113 (1983).

[13]D. Husain and J. Schifino, J. Chem. Soc. Faraday Trans. II **79**, 919 (1983).

[14]M. Czajkowski, E. Walentynowicz, and L. Krause, J. Quant. Spectrosc. Radiat. Transfer **28**, 493 (1982).

[15]D. H. Giers, J. B. Atkinson, and L. Krause, Can. J. Phys. **62**, 1616 (1984).

[16]H. C. Meng and H. J. Kunze, Phys. Fluids **22**, 1082 (1979).

[17]K. P. Selter and H. J. Kunze, Phys. Scr. **25**, 929 (1982). P. Leisman, V. Henč-Bartolič, U. Rebhan, and H. J. Kunze, Phys. Scr. **30**, 186 (1984).

[18]H. L. Bay, B. Schweer, P. Bogen, and E. Hintz, J. Nucl. Mater. **111&112**, 732 (1982).

[19]E. Dullni, Nucl. Instrum. Methods Phys. Res. B **2**, 610 (1984). E. Dullni, Appl. Phys. A **38**, 131 (1985).

[20]W. E. Baylis, J. Chem. Phys. **51**, 2665 (1969).

[21]J. Pascale and J. Vandeplanque, J. Chem. Phys. **60**, 2278 (1974).

[22]J. Pascale, Phys. Rev. A **28**, 632 (1983), and references therein.

[23]J. Cuvellier, P. R. Fournier, F. Gounand, J. Pascale, and J. Berlande, Phys. Rev. A **11**, 846 (1975).

[24]J. M. Mestdaagh, J. Cuvellier, J. Berlande, A. Bivet, and P. De Pujo, J. Phys. B **13**, 4589 (1980).

[25]M. Glodz, J. B. Atkinson, and L. Krause, Can. J. Phys. **59**, 548 (1981).

[26]C. Chaleard, B. Dubreuil, and A. Catherinot, Phys. Rev. A **26**, 1431 (1982).

[27]B. Dubreuil and C. Chaleard, Phys. Rev. A **29**, 958 (1984).

[28]J. Eldward-Berry and M. Berry, J. Chem. Phys. **72**, 4500 (1980).

[29]B. G. Zollars, H. A. Schuessler, J. W. Parker, and R. H. Hill, Jr., Phys. Rev. A **28**, 1329 (1983).

[30]J. W. Parker, H. A. Schuessler, R. H. Hill, Jr., and B. G. Zollars, Phys. Rev. A **29**, 617 (1984).

[31]J. Supronowicz, J. B. Atkinson, and L. Krause, Phys. Rev. A **30**, 112 (1984).

[32]L. Sirko and K. Rosinski, J. Phys. B **18**, L221 (1985).

[33]P. Münster and J. Marek, J. Phys. B **14**, 1009 (1981).

[34]B. Dubreuil, Phys. Rev. A **27**, 2479 (1983).

[35]T. F. Gallagher, S. A. Edelstein, and R. H. Hill, Phys. Rev. A **15**, 1945 (1977).

[36]M. Hugon, F. Gounand, P. R. Fournier, and J. Berlande, J. Phys. B **12**, 2707 (1979).

[37]L. Petitjean, F. Gounand, and P. R. Fournier, Phys. Rev. A **30**, 71 (1984); **30**, 736 (1984).

[38]M. Harnafi and B. Dubreuil, Phys. Rev. A **31**, 1375 (1985).

[39]B. Dubreuil and A. Catherinot, Phys. Rev. A **21**, 188 (1980).

[40]A. Catherinot and B. Dubreuil, Phys. Rev. A **23**, 763 (1981).

[41]A. C. G. Mitchell and M. W. Zemansky, *Resonance Radiation and Excited Atoms* (Cambridge Universiy Press, London, England, 1971).

[42]D. Dezert, Limoges University Report No. 84/1, 1984 (unpublished).

[43]H. Koch and H. J. Eichler, J. Appl. Phys. **54**, 4939 (1983).

[44]W. L. Wiese and J. R. Fuhr, J. Phys. Chem. Ref. Data **4**, 263 (1975).

[45]We observe that the strongest multiplet transition corresponds to the $z\,^3F^\circ_2$–$a\,^3F_2$ (lowest J value) radiative transition, while the theoretically expected multiplet relative line strengths in pure LS coupling should be $S_{4\to4} > S_{3\to3} > S_{2\to2}$. This results from configuration interactions in the titanium atom and leads to departures from pure LS coupling (in Refs. 46 and 47). In particular, for the $z\,^3F^\circ$ energy level under study, the first "leading components" are, respectively, $3d^2(^3F)4s\,4p(^3P^\circ)^3F^\circ$ (88%) and $3d^2(^1D)4s\,4p(^3P^\circ)^3F^\circ$ (8%), according to the data published in Ref. 47.

[46]R. D. Cowan, *The Theory of Atomic Structure and Spectra* (University of California Press, Berkeley, 1981).

[47]Ch. Corliss and J. Sugar, J. Phys. Chem. Ref. Data **8**, 1 (1979).

[48]H. J. Yuh and P. J. Dagdigian, Phys. Rev. A **28**, 63 (1983).

[49]M. H. Alexander, T. Orlikowski, and J. E. Straub, Phys. Rev. A **28**, 73 (1983).